Wind-Generated Equatorial Kelvin Waves Observed Across the Pacific Ocean

C. C. ERIKSEN

Department of Earth, Atmospheric, and Planetary Sciences, Massachusetts Institute of Technology, Cambridge, 02139

M. B. BLUMENTHAL

Massachusetts Institute of Technology–Woods Hole Oceanographic Institution Joint Program in Oceanography, Cambridge and Woods Hole, MA 02543

S. P. HAYES

Pacific Marine Environmental Laboratory/NOAA, Seattle, WA 98105

P. RIPA

Centro de Investigación Científica y Eseñanza Superior de Ensenada (CICESE), Ensenada, Baja California, Mexico

(Manuscript received 23 November 1982, in final form 25 May 1983)

ABSTRACT

Sea-level fluctuations during 1978–80 at equatorial Pacific islands separated by as much as one-quarter of the earth's circumference are coherent at periods of 1–6 weeks with phases implying eastward propagation. Eastward speeds are 16 ± 7.5% higher than expected for a linear, first-baroclinic-mode Kelvin wave (based upon hydrography). Zonal winds in the western Pacific exhibit variation on meridional scales comparable to those of equatorial-ocean baroclinic motions. Roughly one-quarter of sea-level variance in the 1–6 week period range can be explained by local zonal wind alone. The observed admittance magnitude, O[0.1 cm sea level per (m s^{-1})^2 zonal wind pseudo-stress], and phase lag (a few days, sea level lagging wind) can be accounted for in a linear model of baroclinic equatorial Kelvin waves generated by a crudely idealized wind patch of 1000 km zonal scale. Zonal winds at the equator excite, among other things, low-mode Kelvin waves which are recognizable O(10 000 km) to the east of the forcing.

1. Introduction

A unique feature of equatorial oceans is the existence of a free-wave mode of large zonal wavelength which carries energy swiftly to the east, called an equatorial Kelvin mode by analogy with its coastal relative. Moreover, the Kelvin mode can exist in the intermediate range of frequencies between the maximum Rossby and minimum gravity mode frequencies. Kelvin modes are crucial to baroclinic adjustment of an equatorial ocean to changes in atmospheric forcing. They are in large part responsible for the rapid response of equatorial oceans compared to non-equatorial oceans.

Despite their importance to equatorial ocean dynamics, Kelvin waves have been documented only rather recently. At very low frequency [periods O(1 year)], short-vertical-scale deep equatorial jets have been described in part as Kelvin waves (Eriksen, 1981, 1982a). Vertical group velocities of such waves are so small that baroclinic modes are unlikely to be formed since the waves will reach coasts before the ocean bottom. At higher frequencies, baroclinic modes of Kelvin waves are more likely. Because low baroclinic modes produce measurable changes in sea level (e.g., Wunsch and Gill, 1976), Kelvin waves at periods of a few weeks should be detectable in tide-gage records. The Kelvin mode is the only free equatorial wave that produces sea-level changes at the equator in the frequency gap between Rossby and gravity waves for a given baroclinic mode. Rossby modes tend to have relatively little of their total energy manifested as vertical displacement (i.e., sea level) near the equator. As it turns out, together with long-period tides and changes in sea level forced by barometric pressure, Kelvin waves form a prominent part of sea-level fluctuations along the equator in the data we examine.

Observations of Kelvin modes at periods of a few weeks have so far been confined to the Pacific Ocean. Eastward phase speed at nearly the rate expected from linear theory [c_m where $N(z)/c_m$ is the local vertical wavenumber for baroclinic mode m] has been the principal characteristic used to identify motions of "Kelvin wave" type. Luther (1980) was the first to make this identification. He used long sea-level rec-

ords from various different years at islands all across the Pacific basin to find an eastward wavenumber for which the predictions of linear theory were consistent for Kelvin waves in the 35–80 day band. In this band, wavenumbers may differ by more than an octave so that the particular energy distribution of waves in that band may bias the wavenumber estimate. In addition, different years may have different spectral distributions at periods of several weeks, a possibility evident from long wind records (Luther, personal communication, 1982). These two possibilities make precise determination of wavenumber difficult. Knox and Halpern (1982) have documented a burst in integrated upper-ocean zonal current at two sites along the equator in the central Pacific and related it to a subsequent rise in sea level at the Galápagos Islands with which a Kelvin-wave hypothesis is consistent. The single burst in current lasted several days in a record just over 3 months long. Ripa and Hayes (1981) have shown that meridional variation of sea-level energy at periods of a few weeks has a shape not inconsistent with what would be expected for a first-baroclinic-mode Kelvin wave. In examining an array of two years of sea-level measurements in the western Pacific starting in March 1978 (some of the same data used here), we found (Eriksen, 1982b) eastward wavenumbers slightly lower than those predicted by linear theory for equatorial Kelvin waves in frequency bands centered at 1–5 cycles per 40 days (with the exception of the band containing the lunar fortnightly tide). The zonal lags of the island array ranged from 87–2377 km. At the highest frequency these waves were detected, the largest zonal lag corresponds to about one wavelength.

In an effort to examine data taken at longer zonal lags from concurrent data, we combined the sea-level records from the Galápagos Islands with those taken in the Gilbert Group, Republic of Kiribati, for this study. In addition, we obtained concurrent weather records from Gilbert Group locations. These data show statistically significant evidence for Kelvin waves in the first baroclinic mode generated by zonal wind in the western Pacific propagating over more than one-quarter of the earth's circumference. Moreover, these waves travel at speeds somewhat faster than linear theory predicts, suggesting nonlinear effects due to equatorial currents through which they propagate.

In Section 2, the data base and processing procedures for this study are described, followed by observational results of sea level coherence (Section 3), wind structure (Section 4), and coherence between wind and sea level (Section 5). In Section 6, a linear model for the sea-level admittance to zonal stress is developed and compared with the observed admittance. A discussion of related observations of Kelvin-wave propagation and wind forcing as well as concluding remarks appear in Section 7.

2. Data

The basic data for this study are sea-level and weather records from various islands in the Pacific, all within 3° latitude of the equator. The locations of these islands are given in Fig. 1 and details of the records in Table 1. The measurements were taken during various intervals of the 3-year period beginning January 1978.

The sea-level data are from two types of instruments: conventional well-type tide gages mounted in harbors and pressure gages placed at $\sim$10 m depth in lagoons or on coral reefs. The conventional tide-gage records were provided by Prof. Klaus Wyrtki (University of Hawaii). These gages are part of Wyrtki's long-term Pacific sea-level-monitoring network. They require an observer to maintain the gage and send the data in monthly blocks to Honolulu for keypunching and editing. Gaps in these records occur when any of a variety of problems arise with the gage or the observer. The pressure-gage records are from two types of internally recording instruments. The instruments deployed in the Gilbert Group, Republic of Kiribati, were modified temperature–pressure (T/P) recorders (see Wunsch and Dahlen, 1974). The instrument at N. Isabela, described by Hayes *et al.*, (1978), also measures temperature and pressure, but uses a different sensing technique. Pressure gages record a signal that is proportional to sea level plus barometric pressure change. Conventional tide gages measure only sea-level changes. To a large extent, pressure-gage data are considered interchangeably with sea-level data in this work. Some important exceptions are noted where appropriate in the text. With both measurement techniques, the quantity of interest is open-ocean sea-level change (interpreted in this study in part as a manifestation of particular baroclinic-mode equatorial waves).

Some processes may affect sea level at the measurement site that are not indicative of open-ocean changes, but have nearly the same time scales. Principal among these is wave setup due to radiation stresses of surface waves dissipating at the entrance to the harbor or lagoon where sea level is measured. Since the directional spectrum of wind waves varies with changes in wind stress, some correlation locally is expected between sea level and wind stress. At Nauru, for example, this mechanism is responsible for often large (20 cm) sea-level changes that are not found at nearby islands (K. Wyrtki, personal communication, 1982). Another process affecting sea level that is island-specific is island-trapping of various wave modes (e.g., Wunsch, 1972). These waves usually have the fortunate quality of contributing identifiable peaks in the sea-level frequency spectrum. Sea-level signals that are due to local forcing or are locally trapped do not show up in the autospectra and cross-spectra of widely separated islands. Although

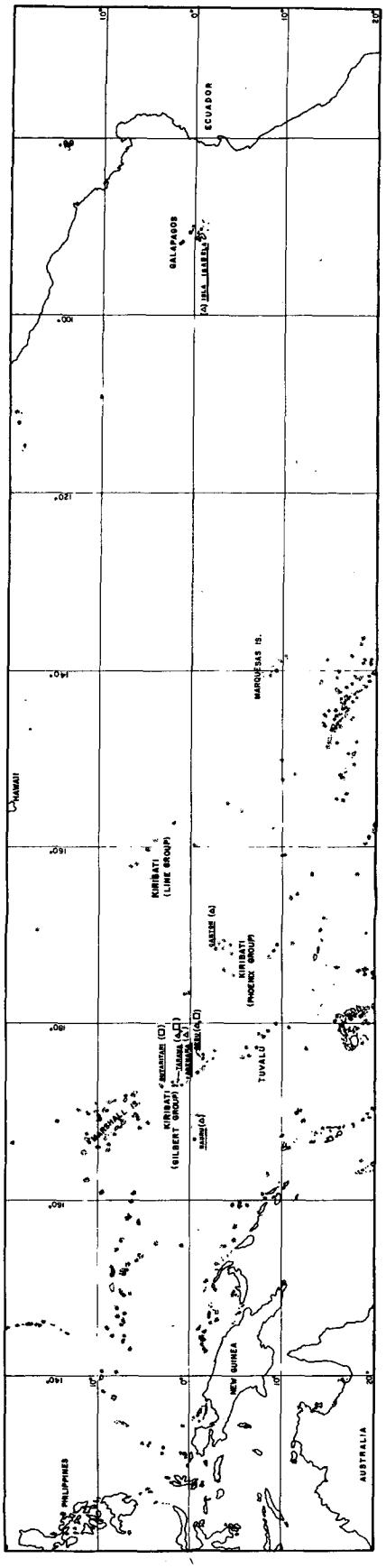

FIG. 1. Locations of island (underlined) tide gages (triangles) and weather stations (squares) used in this study.

in principle the sea-level variance associated with local and nonlocal processes can be distinguished via coherence estimates at different islands, the possibly large scale of wind events and decoherence of sea level between islands due to finite bandwidth and other processes makes this distinction impractical. Rather than try to remove them, it must simply be remembered that the sea-level records considered here are contaminated to some extent by local effects which are not representative of open-ocean fluctuations.

The weather records used in this study consist of tabulations of wind speed, wind direction (to the nearest 15° true azimuth), and barometric pressure at three islands in the Gilbert Group. At two of the islands, Butaritari and Beru, winds were estimated by observing the coconut palms (a technique akin to the Beaufort scale). Observers were first trained in this technique at Tarawa, where the anemometer is mounted 37 m above the ground (12 m above the tops of the trees). These observations were collected under the auspices of the New Zealand Meteorological Establishment to aid in weather prediction for aircraft routing. The raw data were kindly furnished by Dr. Douglas Luther and his co-workers at Scripps Institution of Oceanography. The accuracy of the wind measurements is discussed in Section 4.

The tide-gage data were collected variously at 15, 60 and 64 min intervals, depending on the instrument. Weather records were collected at 3 or 6 h intervals, depending on the station. Only records with gaps of no more than one day in any variable are used here. The gaps were interpolated via tidal prediction in sea level or linear interpolation in weather variables. Weather records were edited to remove obvious spurious data values. Wind records were resolved into eastward and northward components. For computation of spectral quantities, records totaling at least 200 days with pieces no smaller than 120 days were used. Standard techniques of spectral analysis were used, combining frequency-band and data-piece averaging to obtain statistical reliability. Confidence intervals for autospectra and levels of zero significance for coherence were calculated as by Koopmans (1974) according to the number of independent frequency bands and pieces averaged.

A subset of the total data collection from the equatorial Pacific we have on hand was chosen for this study. Records used had to satisfy our criteria for minimum record length, as mentioned previously, be cotemporal with at least one other island station, and be from stations sufficiently separated zonally to yield measurable phase differences between islands in the frequency bands of interest. Several of the sea-level records used by Eriksen (1982b) and by Ripa and Hayes (1981) fail to meet these conditions, and thus were not used here. In addition, the deep temperature and current measurements reported by Eriksen (1982b) were omitted from this analysis because phases of these measurements are contaminated by proximity to the ocean bottom at low frequencies.

TABLE 1. Sea level and weather records used in this study.

Island	Record No.	Latitude	Longitude	Start date	Sampling interval (min)	Duration (days)	Variables measured*	Depth (m)
N. Isabella	—	0°03'S	91°28'W	28-6-79	15	148	*P*	26
		0°03'S	91°28'W	25-11-79	15	361	*P*	26
Canton	—	2°48.6'S	173°43.1'W	1-12-77	15	141	s.l.	—
		2°48.6'S	173°43.1'W	24-4-78	15	82	s.l.	—
		2°48.6'S	173°43.1'W	18-7-78	15	261	s.l.	—
		2°48.6'S	173°43.1'W	6-4-79	15	180	s.l.	—
		2°48.6'S	173°43.1'W	31-10-79	15	78	s.l.	—
		2°48.6'S	173°43.1'W	23-1-80	15	209	s.l.	—
Beru	D0351	1°20'S	176°0'E	8-4-78	64	389	*P*	10.0
	D0461	1°20'S	176°0'E	3-5-79	64	322	*P*	14.1
	91623	1°21'S	176°0'E	1-3-78	360	1006	P_{air}, E, N	−2.0
Abemama	D0371	0°25'N	173°47'E	2-4-78	64	405	*P*	8.4
	D0451	0°25'N	173°47'E	13-5-79	60	319	*P*	8.2
Tarawa	—	1°21.5'N	172°56.0'E	3-5-78	15	359	s.l.	—
	—	1°21.5'N	172°56.0'E	27-6-79	15	70	s.l.	—
	—	1°21.5'N	172°56.0'E	7-11-79	15	82	s.l.	—
	91610	1°21'N	172°55'E	1-1-78	180	731	P_{air}, E, N	−2.0
Butaritari	—	3°02'N	172°47'E	1-1-79	360	1096	E, N	−1.0
Nauru	—	0°31.7'S	166°54.3'E	26-4-78	15	81	s.l.	—
		0°31.7'S	166°54.3'E	27-7-78	15	202	s.l.	—
		0°31.7'S	166°54.3'E	14-2-80	15	320	s.l.	—

* Explanation of symbols:
P = pressure due to barometric pressure plus water at measurement depth.
s.l. = sea level measured by conventional tide gage.
P_{air} = barometric pressure.
E, N = eastward and northward wind components.

3. Sea-level fluctuations at long period

Sea-level records from various near-equatorial island stations considered in this study show fluctuations at periods of a week or longer with amplitudes of about 5–10 cm. Low-passed versions of these records, from which the diurnal and semidiurnal tides were first removed by linear prediction on astronomical forcing, are shown in Fig. 2a. A Gaussian filter with 2-day half-width was used to produce these plots. The most prominent variation is annual, but is not the signal of primary interest in this study. Rather, the fluctuations with periods of about one to six weeks are those for which a clear tendency for eastward propagation can be discerned. At the islands closest to one another zonally, Abemama and Tarawa, fluctuations in this band appear highly correlated at zero temporal lag. Inspection of the records for Nauru and Canton suggest a lead of about 2 days and a lag of about 5 days over Tarawa and Abemama, respectively. The largest lag from Abemama and Tarawa is to N. Isabela, roughly 41 days. These lags were chosen initially by overlaying the low-passed traces and searching visually for the largest apparent correlation. A proper quantitative measure, the coherence phase behavior with frequency in this band, corroborates these visual impressions, as will be discussed.

In Fig. 2b, the same low-passed records have been plotted with the various lags discussed here accounted for in such a way as to reference them all to Abemama and Tarawa. It is clear from these adjusted traces that a substantial fraction of the variance at periods of a few weeks is coherent between these records which span more than 100° of longitude. The similarity between the Abemama and adjusted N. Isabela trace is unmistakable, yet these records were taken more than one-quarter of the earth's circumference apart. The particular event which occurs about 1 April 1980 in the Gilbert Group (a sharp rise in sea level which occurs simultaneously in the lag-adjusted records of Nauru, Abemama, Canton and N. Isabela) has been observed in current meter records at 153 and 110°W by Knox and Halpern (1982). The traces in Fig. 2b suggest that this event was not an isolated feature in sea level, but that such events are commonplace with lesser amplitude. These events are reminiscent of the spectral results of a sea-level study by Luther (1980). He reports significant coherence with eastward phase in a 35–80 day period band between islands as far west as Christmas Island (157°30'W, 2°N) and the Galápagos Islands which he identified tentatively as a Kelvin wave on the basis of inferred phase speeds.

The records we have are generally shorter than those Luther used, yet they show much the same result at somewhat higher frequency. Examples are

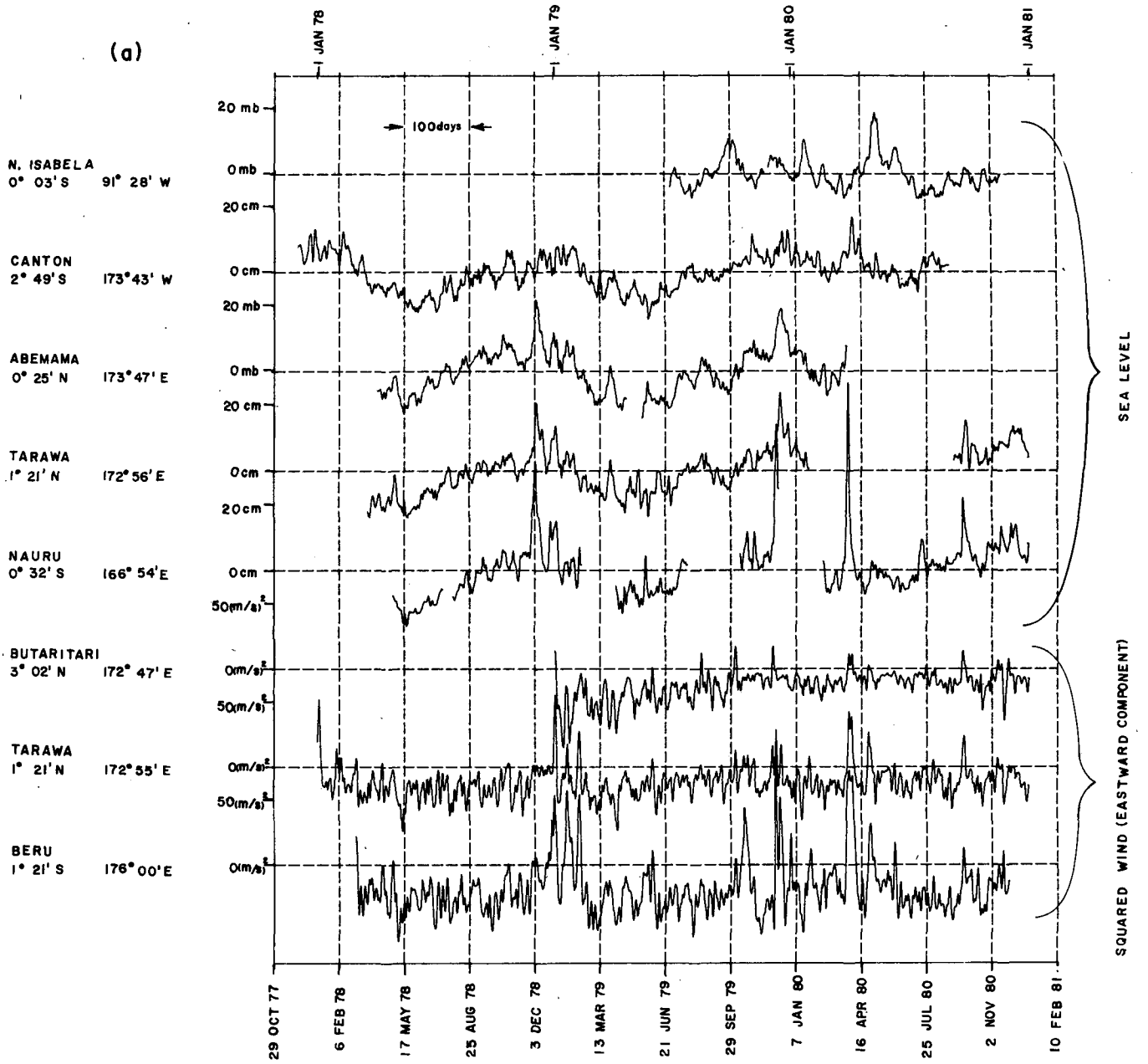

FIG. 2. (a) Time series of sea level and eastward pseudo-stress from various island stations during the three years 1978–1980. Records have been low-pass filtered with a Gaussian of 2-day half-width. (b) Time series adjusted by lags implied by coherence phases to match the records at Abemama and Tarawa. Thin vertical lines have been drawn to call attention to particularly prominent peaks in sea level and eastward pseudo-stress which appear concurrent when referenced to Abemama and Tarawa.

given in Fig. 3a based on 200–320 days of records. In each case, coherence magnitude is only barely above or actually below the 95% level of zero significance for estimates in the first three frequency bands (1–3 cycles per 40 days). However, phases vary in these bands in a manner consistent with a constant time lag between them; that is, the phases appear to vary linearly with frequency. The phase changes with frequency imply the lags found visually in the low-passed traces discussed above. The estimates given are based on the mean value of observed phase divided by frequency for the first three frequency-band estimates (1–3 cycles per 40 days). Estimates of the confidence intervals for this constant-lag model are given by $\pm SN^{-1/2}t_{N-1,\alpha/2}$, where S is the sample standard deviation of lag, t Student's t distribution, $N = 3$ is the number of independent frequencies used in the estimate, and $\alpha/2 = 0.025$ for 95% confidence

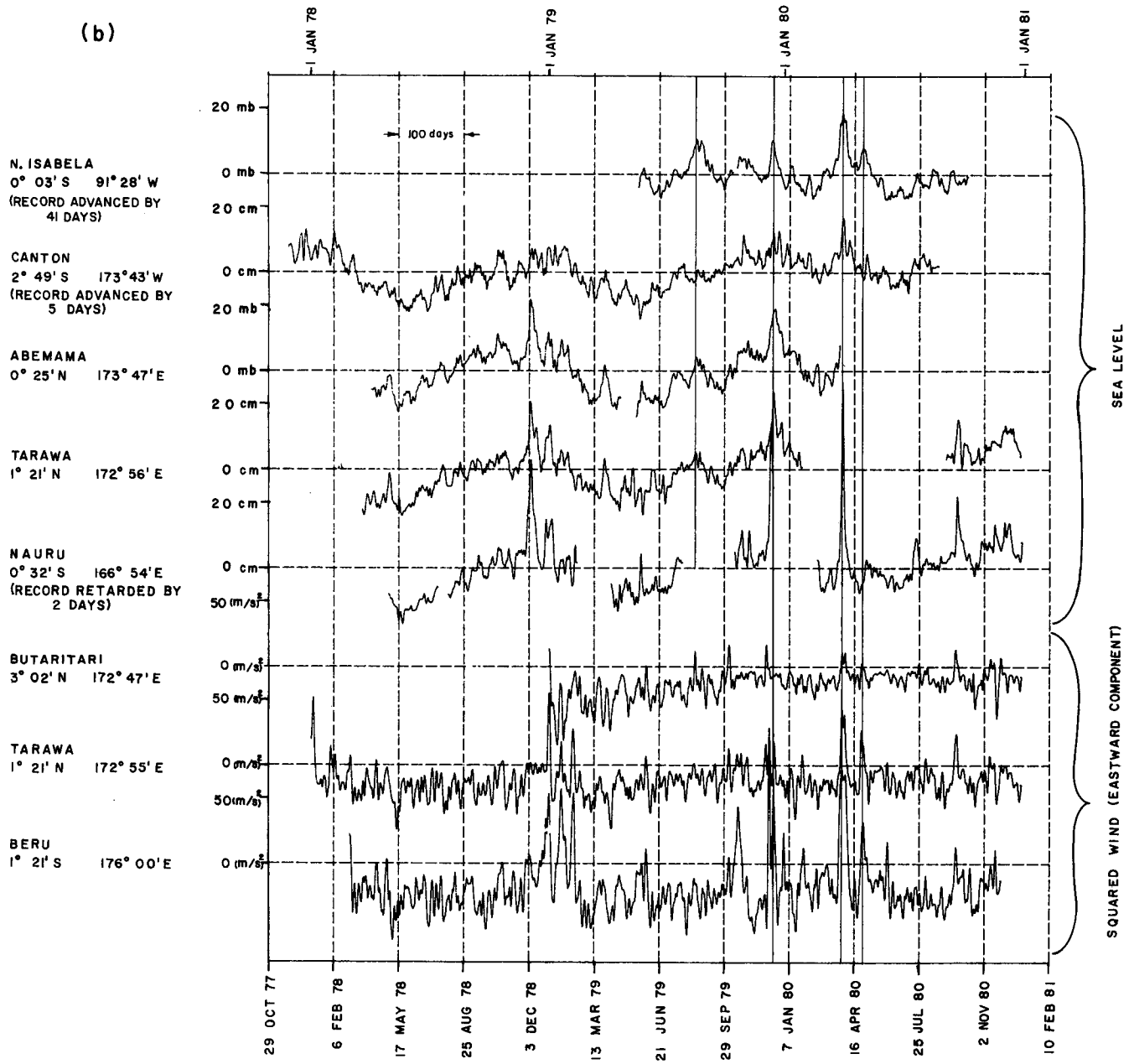

FIG. 2. (*Continued*)

(Bendat and Piersol, 1971). The mean and 95%-confidence intervals for the constant-lag model are given in Fig. 3a for the three island pairs for which enough data were available to make a statistically significant (nonzero) lag calculation. Frequencies higher than 3 cycles per 40 days did not agree with the constant-lag model for the two largest separations. For the smallest separation (Nauru-Canton), using the first six frequency-band estimates (1–6 cycles per 40 days) gives a lag of 7.36 ± 0.66 days as compared with 7.18 ± 1.76 days for the first three bands only.

Although the lags calculated in Fig. 3a are from a mixture of sea-level and subsurface pressure records (i.e., the sum of sea-level and barometric contributions to pressure), the results are self-consistent, showing a relatively smooth variation of zonal speed with longitude, regardless of whether lags were calculated from a pair of sea-level records, a pair of subsurface pressure records, or one record of each kind. As will be noted below, barometric pressure is incoherent with sea level (but significantly coherent with subsurface pressure) at islands for which both weather

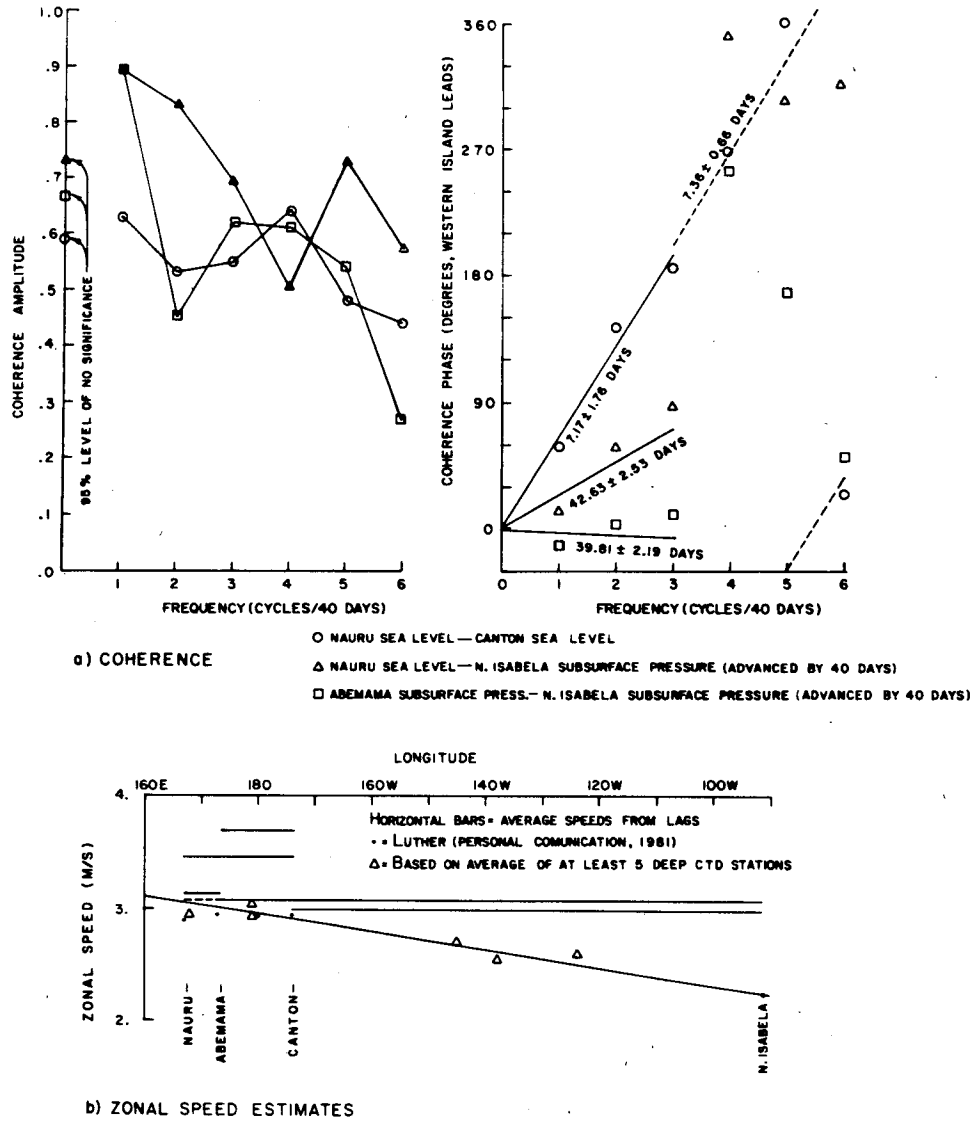

FIG. 3. (a) Coherence magnitude and phase of sea level between various island stations near the equator. The zero significance levels at 95% confidence in magnitude are indicated with thin horizontal lines. Least-squares regressions of phase, constrained to be zero at zero frequency, are indicated with thin lines, along with the implied time lags. In all cases, the western island leads the pair. Listed with the lags are their 95% confidence intervals (discussed in text). (b) Zonal speeds computed from linear theory applied to observed hydrographic structure plotted against longitude. Horizontal bars indicate average speeds computed from sea level at various island pairs. A least-squares regression against the hydrography-predicted speeds is indicated by the sloping line. Triangles indicate speed estimates based on high-quality CTD profiles; dots indicate estimates derived by Luther (1980) from atlas data.

data and sea-level (Tarawa) or subsurface pressure (Beru) are available.

These lag relationships can be interpreted as average phase speeds or, more precisely, as inverted average inverse speeds between the various island pairs. Fig. 3b summarizes these speed estimates by horizontal bars drawn between longitudes of the islands for which a lag was estimated. For reference, the local linear Kelvin-wave phase speed c_1 (first baroclinic mode) calculated from hydrography is indicated for several locations. The triangles indicate calculations based on averages of 5–11 high-quality CTD (conductivity–temperature–depth) profiles to the ocean bottom taken within one or two weeks of one another. The dots are additional calculations based on seasonally averaged atlas data in the upper 500 m and an exponential buoyancy-frequency profile below (Luther, personal communication, 1981).

A least-squares fit to all ten estimates for the first-baroclinic-mode phase speed is indicated in Fig. 3b by the sloping line. The speeds decline from a maximum of nearly 3.00 m s^{-1} near the Gilbert Group to about 2.25 m s^{-1} near the Galápagos Islands. West of the Gilberts speeds again decline (Luther, personal communication, 1981). The speeds are roughly proportional to ocean depth times average buoyancy frequency.

Since the time lag of a wave traveling at speed $c(x)$ between $x = x_1$ and $x = x_2$ is

$$t = \int_{x_1}^{x_2} \frac{dx}{c(x)},$$

the average speed inferred over this separation is $\bar{c} = (x_2 - x_1)/t$. If $c(x)$ is taken to be the simple linear function plotted in Fig. 3b, the model-average speed for the interval (x_1, x_2) is $\bar{c} = [c(x_2) - c(x_1)]/\ln[c(x_2)/c(x_1)]$. A comparison of the observed speeds with those expected from hydrography and linear theory gives the result that observed speeds exceed model speeds by an average of 16 ± 8% (at 95% confidence) based on the data and model $\bar{c}(x)$ shown in Fig. 3b; that is, the process which governs the propagation of sea-level variations to the east at periods of a few weeks is significantly faster than a linear Kelvin wave.

The long-period tides are a major source of sea-level variance in the frequency bands considered here. The two principal constituents are the lunar monthly (Mm) and lunar fortnightly (Mf) tides. These have amplitudes in the equatorial Pacific of roughly 0.5–1.0 and 1.0–1.5 cm, respectively, according to Luther (1980). Together, they account for roughly one-third of the variance in sea level in the 1–3 cycle per 40 day band (see Fig. 7 for typical sea-level spectra), and thus might bias the zonal-speed estimates given here. These tides are nearly in equilibrium and, just as their forcing, have no discernable zonal scale (Luther, 1980). Their vanishing zonal wavenumber compared to that of an oceanic Kelvin wave ($k = \omega c^{-1}$) causes them to contaminate but not systematically bias zonal-lag estimates.

A simple model of coherence–phase behavior computed between two islands where a Kelvin wave of unit amplitude and a tide of amplitude a account for all the sea-level signal will illustrate the type of contamination expected. On the assumption that the oceanic Kelvin wave and the tide are randomly phased with respect to one another, the coherence over a distance d is

$$[\exp(ikd) + a^2 \exp(iKd)](1 + a^2)^{-1},$$

where K is the zonal wavenumber of the tide. The coherence phase θ of sea level is then

$$\theta = \arctan\left\{\frac{[\sin(\omega d/c) + a^2 \sin Kd]}{[\cos(\omega d/c) + a^2 \cos Kd]}\right\}$$

This phase increases linearly with $\omega d/c$ for $a^2 = 0$ (the interpretation we have made in Fig. 3a), but at a faster or slower rate depending on $a \neq 0$ (but $a < 1$) and Kd. The maximum difference δ between θ for $a = 0$ and $a \neq 0$,

$$|\delta \text{ max}| = \arcsin a^2$$

occurs when $\cos\omega d/c + a^2 \cos Kd = 0$. For separations d that do not satisfy this condition at tidal frequencies, the deviation from θ is smaller. For a^2 as large as 0.5, $|\delta \text{ max}| = \pi/12$, but the average value for δ is zero (an average over different values of $\omega d/c$). Although individual estimates of θ for a given separation d may be contaminated, its average behavior over several frequency bands is $\omega d/c$ for $a < 1$. At the frequencies Mm and Mf, the separations used in Fig. 3a imply $\pi/2 \leqslant \omega d/c \leqslant 6\pi$. (For the two longer separations, the lag ωT (T = 40 days) imposed in the calculation is subtracted from these phases.)

A similar argument pertains to lags θ calculated from pairs of subsurface-pressure records used as sea-level records, since barometric pressure disturbances may be coherent over large zonal separations. Luther (1980) estimated the zonal wavenumber of pressure disturbances to be between ±1 cycle per earth circumference in the frequency band of interest. Although Kd is not so small as for long-period tides, it is still small compared to $\omega d/c$ in the ranges of interest. As shown in Fig. 7, an appropriate value for a is ~0.25, so $|\delta \text{ max}| = 15°$. Again as with tides, although this contamination will introduce noise in individual estimates of θ, its average behavior over a frequency band is still $\omega d/c$.

Both tides and barometric pressure may alter individual phase estimates somewhat, but they do not bias the calculation of zonal speed of the Kelvin wave. Evidence for the lack of contamination of the sea-level coherences by these effects is the rather small standard deviations of observed phases about the constant lags listed in Fig. 3a and discussed in a previous paragraph.

4. Structure of the winds

The wind data used in this study were collected in a somewhat novel manner, as mentioned in Section 2, so their representativeness needs to be established. There are several potential problems concerning the measurement technique, but, as will be shown here, the overall patterns are believable even though determination of actual wind-stress magnitude at the sea surface is in some doubt. The spectra of east and north wind at the three island stations (Butaritari, 3°02′N, 172°47′E; Tarawa, 1°21′N, 172°55′E; Beru, 1°21′S, 176°0′E) share similar features and amplitudes, particularly at high frequencies, which suggests that they are mutually consistent. These spectra (see Fig. 4) vary roughly with the −4/5 power of frequency

at periods shorter than ~1 week, as indicated by the sloping reference level. This reference is the one chosen by Luther (1980); the spectra in Fig. 4 have levels commensurate with those shown by Luther at other tropical Pacific islands. Thus, although the winds at Beru and Butaritari were estimated from behavior of the coconut palms, their spectra suggest that they are as representative as anemometer winds at Tarawa of open-ocean winds.

The anemometer at Tarawa is mounted on a mast 37 m above the ground (2 m above sea level), 12–15 m above the tops of the coconut palms. The precise relationship between these winds and wind stress over the open ocean is unknown. Simple logarithmic correction of the 37 m to 10 m winds, according to a constant stress assumption for use in an aerodynamic drag law to compute stress, seems overly simple because of the possible effects of the island or coconut palms. Nevertheless, such a correction implies a 12% reduction in wind speed from the 37 m to the 10 m level. However, the palm trees may act as a forest canopy, making the situation more complicated (Tajchman, 1981).

At neither Tarawa nor Beru, where barometric pressure and winds are both available, is either wind component coherent with barometric pressure at low

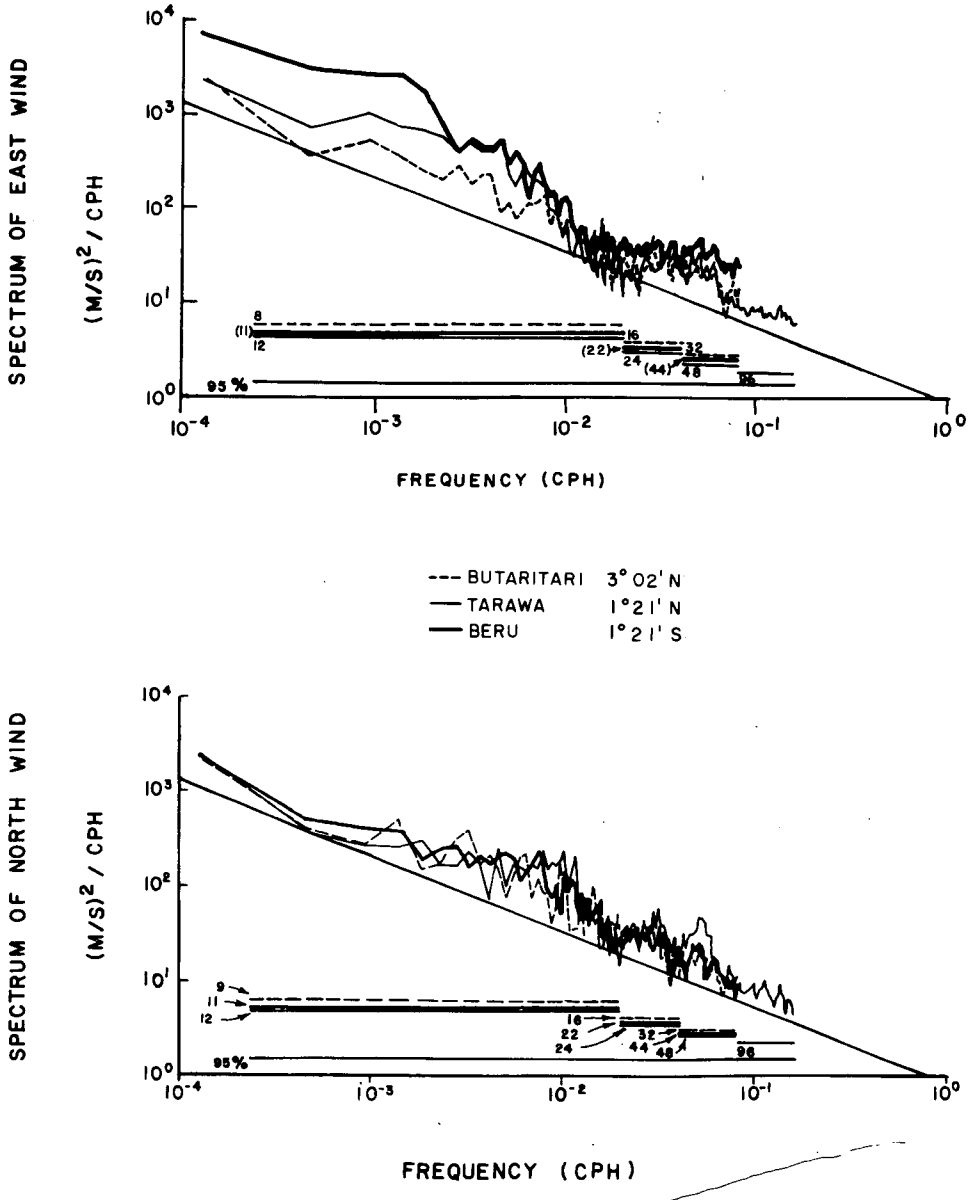

FIG. 4. Autospectra of east and north wind from Butaritari, Tarawa and Beru. Reference level with −4/5 frequency slope is that used by Luther, 1980.

frequencies (1–9 cycles per 90 days). Thus, when considering coherence of winds or barometric pressure with sea level or subsurface pressure, the two may be regarded as independent types of potential forcing in this band. The two wind components are only marginally coherent with each other at the same island. At Beru, coherence between the two rotary components of the wind is significantly nonzero at these low frequencies. (At Tarawa, rotary coherence is marginal in this band.) At both islands, the principal axis of the wind over the 1–9 cycle per day band is oriented 12° south of east, whereas the mean wind comes from 8° north of east. So, although the mean wind appears to be a northeast trade wind, the low-frequency fluctuations have a "southeast-trade-wind-like" character of about half the energy in the mean.

The interesting feature in the winds is structure on the scale of oceanic structure. The spectra of east wind clearly indicate an increase in energy at periods longer than about a week from Butaritari south to Beru. The spectrum of Tarawa east wind exceeds that for Butaritari by a factor of 2–3 for periods between about one week and three months, and the spectrum of Beru east wind exceeds that for Tarawa by another factor of 3 or so at periods between three weeks and three months (Fig. 4). No such geographical change is apparent in the north wind at the three islands. The east wind spectrum at Butaritari, the island closest to the Intertropical Convergence Zone (ITCZ), is indistinguishable from spectra of north wind for all three islands. Low-frequency fluctuations in wind are strongest at the island farthest from the ITCZ (as is evident from the low-passed records in Fig. 2), with a pronounced zonal character.

The meridional coherence scales of the wind are of the order of the separation of the islands. The coherence of zonal wind at neighboring islands is high at low frequencies, but only marginally significant over the largest separation. The coherences plotted in Fig. 5a show this pattern where the shortest separation (Tarawa to Butaritari, 187 km meridionally, 15 km zonally) is generally less coherent than the larger separation between Tarawa and Beru (300 km meridionally, 343 km zonally). Over the largest separation, between Beru and Butaritari (487 km meridionally, 357 km zonally), coherence is at most barely significant at only a few frequency estimates. Where coherences are significantly nonzero, the phase estimates are indistinguishable from zero suggesting symmetry across the equator. Coherence of north wind is somewhat lower at these separations than for east wind. As with east wind, north winds at Beru and Butaritari are only marginally coherent. Moreover, north winds at Tarawa and Butaritari also are only marginally coherent and north winds at Tarawa and Beru are strongly coherent only at periods longer than about three weeks. The coherent north-wind fluctuations between Tarawa and Beru are the same structures which make zonal wind highly coherent at these two islands. In other words, the energetic low-frequency fluctuations near (and on the south side of) the equator are predominantly, but not exclusively, zonal. One source of such fluctuations may be tropical cyclone pairs which straddle the equator to create largely zonal perturbations to the mean trade winds (Sadler and Kilonsky, 1981; Keen, 1982).

5. Coherence of weather variables with sea level

The coherence of weather variables with local sea-level changes can be examined to determine how much, if any, sea-level variance can be accounted for by local forcing by the atmosphere. Our attention is focused on low frequencies, where, from the zonal coherences of sea level, Kelvin-wave propagation seems evident. The island for which wind variance is strongest is Beru, so it will be used as an example here. The coherences of eastward component of squared wind $[u(u^2 + v^2)^{1/2}]$ in conventional notation, which we shall call east pseudo-stress to avoid specifying a drag coefficient), north pseudo-stress and barometric pressure with sea level are given in Fig. 6. East pseudo-stress is most coherent with sea level at periods longer than about one week (Fig. 6). The coherence magnitude suggests that roughly 25% of the local sea-level variance in the period band 1–6 weeks can be explained by the zonal wind alone. Phase variation is nearly linear with frequency, corresponding to a lag of ~2.5 days between east wind and sea level. By contrast, north pseudo-stress (Fig. 6) is significantly coherent with sea level in only a few isolated frequency bands, notably periods of 8 days and 4 days. The latter period is that at which one of the equatorial gravity modes is prominent in sea level data (see Eriksen, 1982b). Barometric pressure (Fig. 6) is coherent with sea level (subsurface pressure) in the lowest resolvable band (1 cycle per 40 days) and its phase remains zero at periods as short as one week. Zonal wind stress appears to be the principal meteorological contributor to sea level locally. Presumably, the rest of sea-level variance at low frequencies is remotely generated.

At this point, it is appropriate to remind the reader that three of the "sea level" records used here (N. Isabela, Beru and Abemama) are really records of subsurface pressure (i.e., the sum of barometric pressure and pressure due to sea level measured in a shallow lagoon). Autospectra of two such subsurface pressure records appear in Fig. 7 along with barometric pressure at Beru. In the band of frequencies over which phase propagation in sea level is observed (Fig. 3), barometric pressure represents about 20% of the subsurface pressure variance. Coherence at low frequency between barometric and subsurface pressure at Beru appears attributable to the fact that one mea-

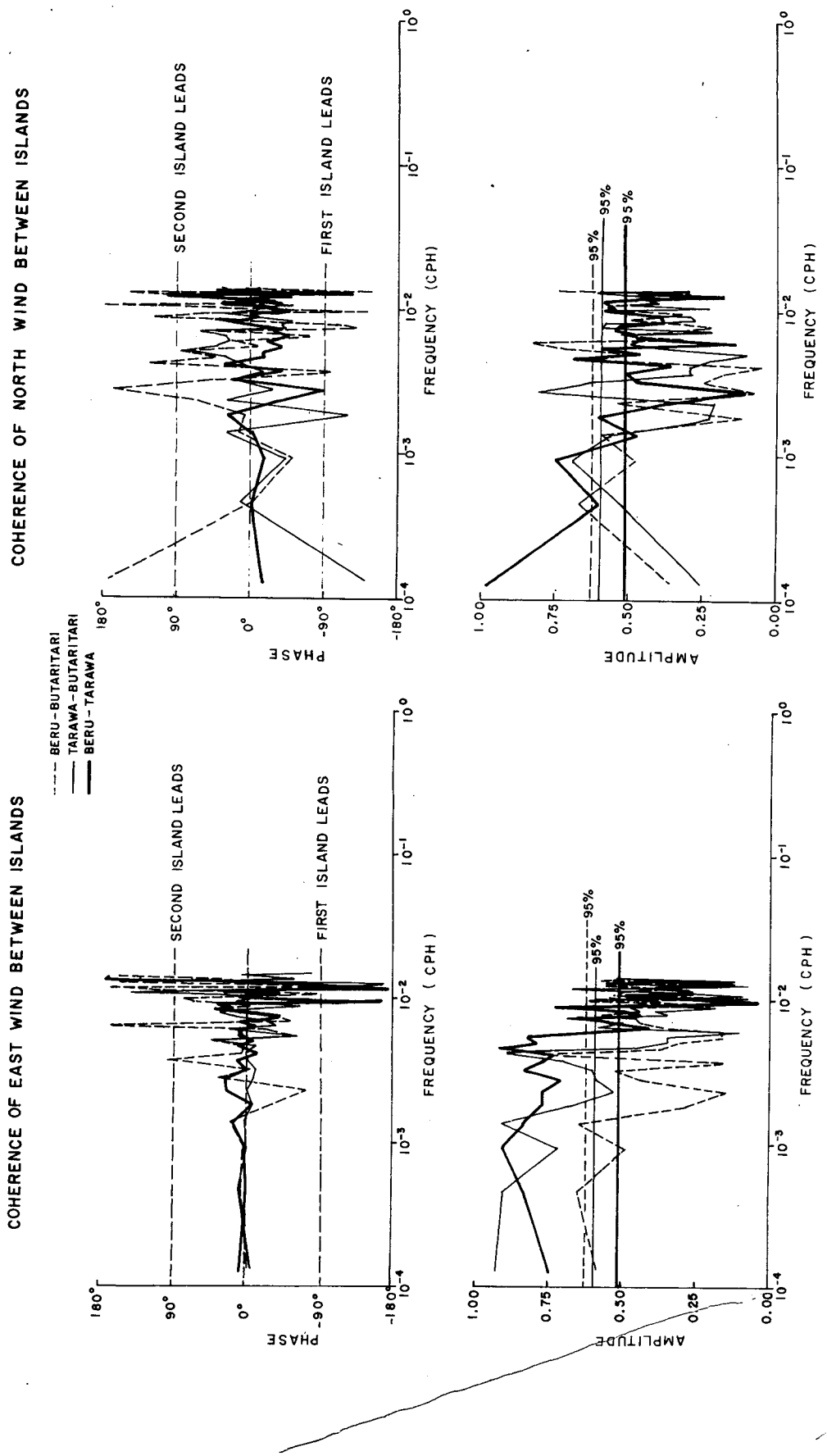

FIG. 5. Coherence of east and north winds between different island pairs.

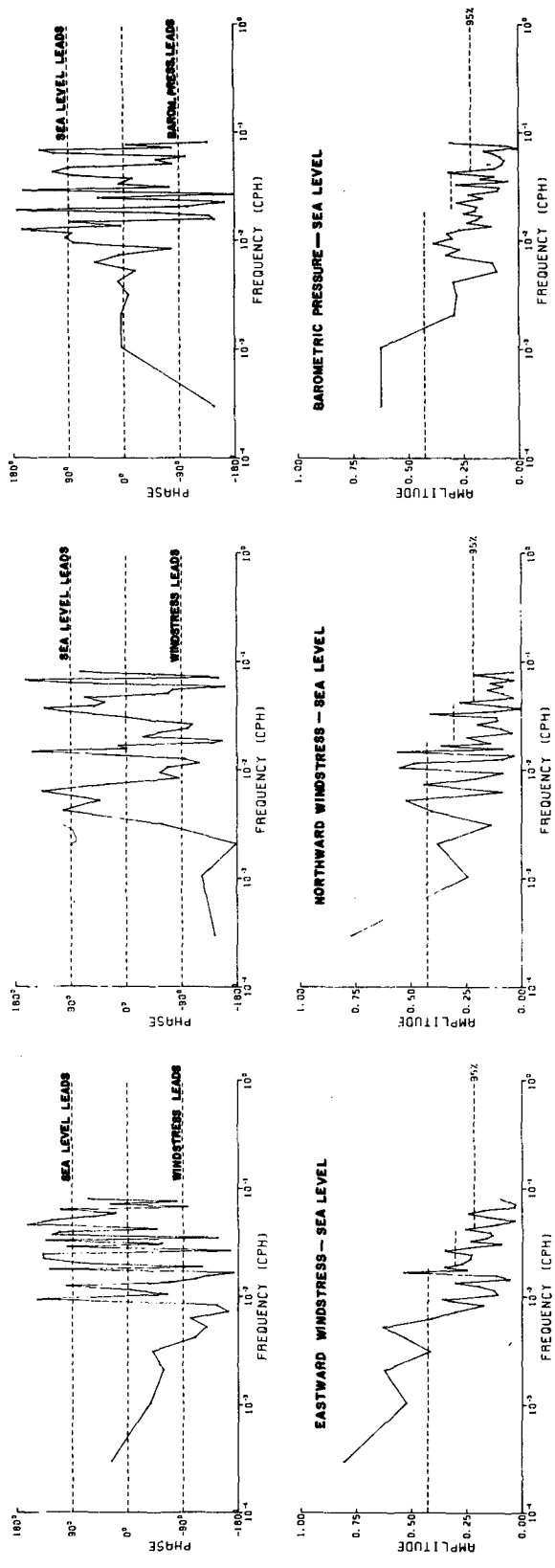

FIG. 6. Coherence at Beru of sea level (actually subsurface pressure) with east pseudo-stress, north pseudo-stress and barometric pressure.

surement contains the other. At Tarawa, where barometric pressure and sea level (not subsurface pressure) records exist, there is no significant coherence between the two at these low frequencies.

Eastward pseudo-stress "events" are apparent in the low-passed records (Fig. 2b) which correspond to sea level events. The particular event studied by Knox and Halpern (1982) corresponds to a reversal of the trade winds in the Gilbert Group about 1 April 1980. Other prominent trade-wind reversals (which are particularly strong at Beru, as expected from the spectra) lasting a few days or so correspond to sea-level peaks locally and at sites to the east occur in January–February, October and December 1979. Not all trade-wind reversals in the Gilbert Group have corresponding peaks in sea level. The zonal scale of each reversal is not known, so some may be more efficient at generating Kelvin waves than others. Luther (personal communication, 1982), on the basis of much longer records, finds that 1979 and 1980 have more of these trade-wind-reversal events than most other years, so that sea level variance in the 1–6 week period band may be higher in the records considered here than in other years.

The pattern which emerges is that sea-level variance is created locally by zonal winds at low frequencies, which then propagates eastward in a manner similar to an equatorial Kelvin wave of lowest baroclinic mode. This means that at least part of the variance in sea level at islands far to the east should be explained by east-wind variance in the Gilbert Group. As an example, Fig. 8 shows the coherence between east pseudo-stress at Beru and sea level at N. Isabela (advanced by 40 days). Coherence is significant only in the 40-day period band, but is significant at less than 95% confidence in both of the next two higher frequency bands. The lag suggested by phase variation is about 43 days; that is, the sum of the lag between forcing and sea level at Beru and the lag between Beru and N. Isabela which corresponds to oceanic propagation. Although, based on data taken in earlier years, Luther (1980) found no atmospheric fluctuations that were coherent over this large zonal separation in this frequency range at such large lag, a result which does not contradict the hypothesis that zonal winds force oceanic Kelvin waves in the western Pacific which propagate east to the Galápagos Islands. Hypotheses involving forcing by other weather variables (e.g., north wind or barometric pressure) can be ruled out, since there is no significant coherence between them and sea level either locally (i.e., in the Gilbert Group) or remotely (at the Galápagos Islands).

6. A linear model of Kelvin-wave generation

In order to test the hypothesis that zonal-wind-stress fluctuations generate equatorial Kelvin waves

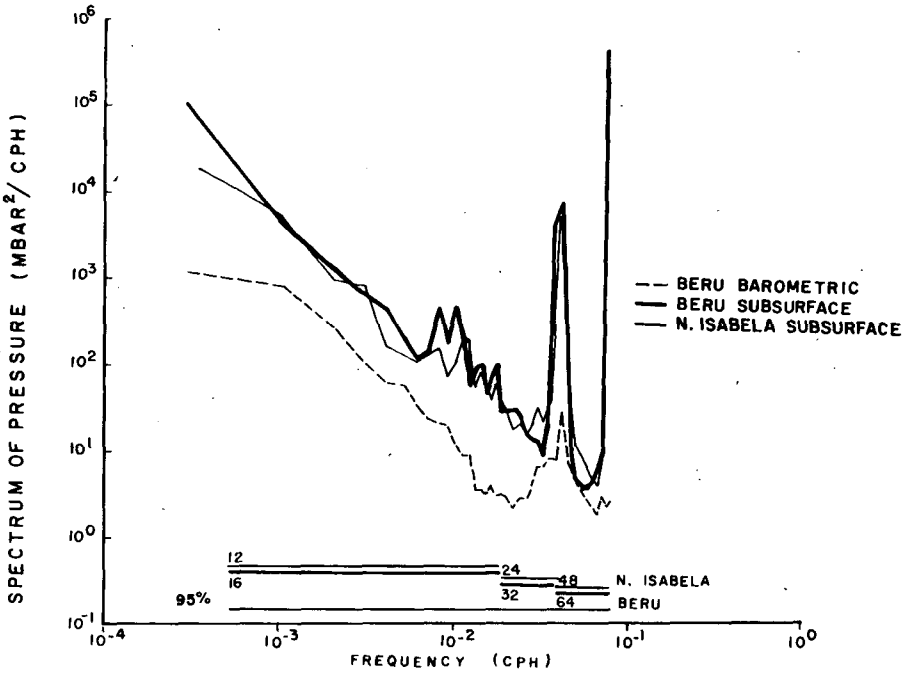

FIG. 7. Autospectra of barometric pressure at Beru and subsurface pressure (sea level plus barometric pressure) at Beru and N. Isabela.

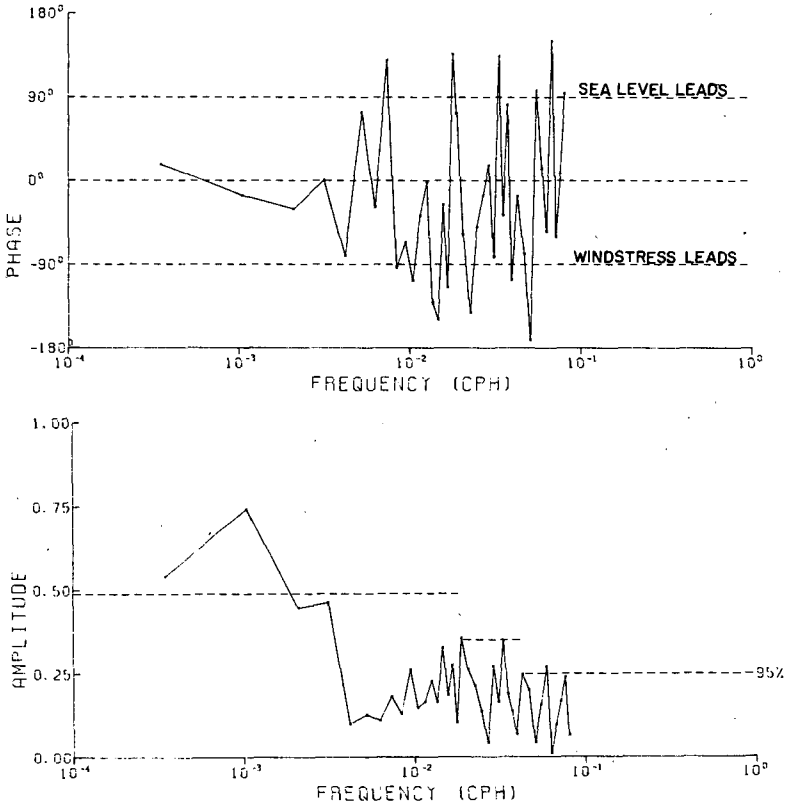

FIG. 8. Coherence of Beru east pseudo-stress with N. Isabela sea level (with the N. Isabela record advanced by 40° to increase the effective overlap of the records).

of low baroclinic mode, an admittance function $a(f)$ can be calculated from the observations and compared to a model admittance calculated from theory. The observed admittance can be calculated from the coherence and autospectra of zonal squared wind and sea level (following Wunsch, 1972) as

$$a(\omega) = \mathrm{coh}(s, \eta)(\Phi\eta/\Phi s)^{1/2},$$

where s is zonal pseudo-stress, η sea level, and Φx the frequency spectrum of x. The phase of $a(\omega)$ is the same as that of $\mathrm{coh}(s, \eta)$, which is shown in Fig. 6a; its magnitude is plotted in Fig. 9c, for comparison with the model. Our goal here is to account for the approximate 2.5-day lag between zonal pseudo-stress and local sea level, and the admittance magnitude of order 0.1 cm sea level per 1 m^2s^{-2} of zonal squared wind.

The mathematical interpretation of admittance is that it is the Fourier transform of the impulse response of a linear system. The response to steady forcing switched on at time $t = 0$ of a linear baroclinic resting equatorial ocean has been worked out by Cane and Sarachik (1976). In general, their technique uses the free modes of the equatorial β-plane to describe response to arbitrary forcing. Their result can be differentiated once and Fourier-transformed in time to find a theoretical admittance. This is particularly easy for Kelvin modes. The frequency range of interest in the observations corresponds to the "spectral gap" between the minimum gravity-wave and maximum Rossby-wave frequencies for low baroclinic modes. For a given amount of energy, low baroclinic modes have much stronger sea-level expression than higher baroclinic modes. Furthermore, vertical displacement for Rossby modes is relatively weak near the equator. In the "spectral gap", the only free waves are the Kelvin and Rossby–gravity modes, the latter having vanishing vertical displacement at the equator. Thus we can expect that low-mode Kelvin waves will provide the strongest signal in the "spectral gap". Table 2 summarizes the scales associated with baroclinic modes based on buoyancy–frequency profiles at 179°E. If the first three modes contribute most of the sea-level signals, as will be demonstrated later (they contribute 71% of the sea-level-response amplitude of the lowest 9 modes), the spectral gap covers effectively periods of ~1–6 weeks. Thus it would not be surprising if the signals apparent in the data at these periods were due to Kelvin waves. We shall concentrate on computing Kelvin-wave response (and its sea-level manifestation) to zonal wind stress.

Rather than ask the question, What equatorial waves does a zonal wind excite?, we ask the narrower question, What Kelvin waves are excited by a zonal wind? A non-dimensional answer is obtainable in a straightforward manner from Cane and Sarachik [1976; Eq. (47) differentiated combined with Eq. (41a)], but for the sake of clarity, we give a more narrow derivation that concentrates on Kelvin waves and includes all the details necessary to make a quantitative comparison between theoretical and observed admittance.

The truncated set of equations that admits only baroclinic Kelvin waves in a linear, Boussinesq, inviscid, incompressible flat-bottomed equatorial β-plane ocean forced by zonal wind stress is:

$$u_t + p_x = f^x/h, \tag{1a}$$

$$\beta y u + p_y = 0, \tag{1b}$$

$$u_x + w_z = 0, \tag{1c}$$

$$N^2 w + p_{zt} = 0, \tag{1d}$$

where p is perturbation reduced pressure, $N(z)$ is buoyancy frequency, and wind stress is applied as body force f^x exerted in a shallow (mixed) layer of depth h near the surface. We look for solutions that are separable in the vertical and horizontal directions:

$$[u, w, p] = \sum_m [u^*_m(x, y, t)G'_m(z), w^*_m(x, y, t)G_m(z), p^*_m(x, y, t)G'_m(z)], \tag{2}$$

where $G_m(z)$ and $G'_m(z)$ are the baroclinic structure functions for vertical and horizontal current [see Eriksen (1980) for details, and Eriksen (1982b) for examples of these functions in the equatorial Pacific]. They are normalized so that

$$\frac{1}{D}\int_{-D}^{0} G'_m(z)G'_n(z)dz = \delta_{mn}, \tag{3}$$

where D is the ocean depth. Projecting the forcing f^x/h onto the baroclinic modes gives

$$F^x_m(x, y, t) = \frac{1}{D}\int_{-D}^{0} \frac{f^x}{h} G'_m dz = \frac{1}{D} f^x G'_m(0), \tag{4}$$

where G'_m is taken as constant in the mixed layer $-h \leqslant z \leqslant 0$. Dropping the asterisks and subscripts after projecting the modes $G'_m(z)$ on Eq. (1), we note the horizontal problem for a particular mode m characterized by the separation constant c:

$$u_t + p_x = F^x, \tag{5a}$$

$$\beta y u + p_y = 0, \tag{5b}$$

$$c^2 u_x + p_t = 0. \tag{5c}$$

The part of F^x that will excite Kelvin waves is that which can be projected on the meridional structure function specified by Eq. (5b) when $u = p/c$:

$$u(x, y, t) = p(x, y, t)/c \propto \exp(-\beta y^2/2c). \tag{6}$$

Then an equation for

$$q(x, t) = [u(x, t) + p(x, t)/c] \exp(-\beta y^2/2c)$$

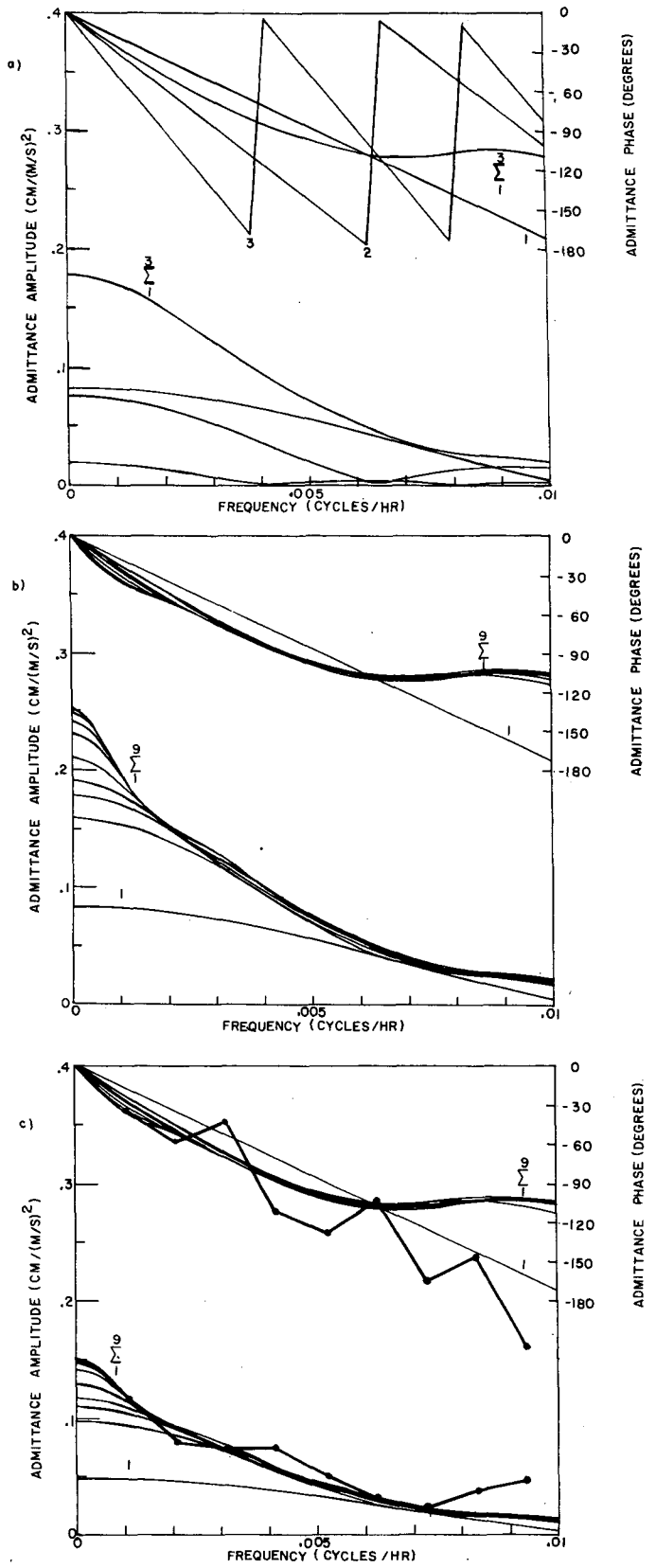
a)
ADMITTANCE AMPLITUDE (CM/(M/S)²)
ADMITTANCE PHASE (DEGREES)
FREQUENCY (CYCLES/HR)
b)
ADMITTANCE AMPLITUDE (CM/(M/S)²)
ADMITTANCE PHASE (DEGREES)
FREQUENCY (CYCLES/HR)
c)
ADMITTANCE AMPLITUDE (CM/(M/S)²)
ADMITTANCE PHASE (DEGREES)
FREQUENCY (CYCLES/HR)

TABLE 2. Baroclinic mode scales, (Computed from CTD casts at 179°E).

Mode No.	Speed c_m (m s^{-1})	Horizontal scale $(c_m/\beta)^{1/2}$ (km)	Frequency scale $(\beta c_m)^{1/2}$ (cpd)	Maximum gravity period (days)	Minimum Rossby period (days)
1	2.91	357	0.112	5.2	30.4
2	1.78	279	0.088	6.7	38.9
3	1.13	222	0.070	8.4	48.9
4	0.827	190	0.060	9.8	57.1
5	0.649	169	0.053	11.1	64.5
6	0.568	158	0.050	11.8	68.9
7	0.471	144	0.045	13.0	75.7
8	0.415	135	0.042	13.8	80.6
9	0.357	125	0.039	14.9	86.9

can be found from (5a) and (5c), i.e.,

$$(\partial t + c\partial x)q(x, t) = (\beta/c\pi)^{1/2} \int_{-\infty}^{\infty} F^x(x, y, t) \times \exp(-\beta y^2/2c)dy = F^{\text{Kelvin}}(x, t). \quad (7)$$

This one-dimensional wave equation can be solved by integrating along characteristics:

$$q(x, t) = \int_{-\infty}^{t} F^{\text{Kelvin}}[x - c(t - t'), t']dt'. \quad (8)$$

In principle, this integration can be done for quite general forcing $f^x(x, y, t)$. Gill and Clarke (1974) and others have used this approach extensively.

To go farther, we need to choose a form for the stress $f^x(x, y, t)$. For simplicity, we choose it to be separable in all three variables, though this choice is not a good characterization of translating storms which may contribute some of the zonal wind variance in the frequency band of interest. Taking $S(t) \cdot X(x/L_x) \cdot Y(y/L_y)$ to be the equivalent squared-wind zonal component, and $(\rho_a/\rho)C$ to be the appropriate drag coefficient,

$$f^x(x, y, t) = (\rho_a/\rho)C \cdot S(t) \cdot X(x/L_x) \cdot Y(y/L_y), \quad (9)$$

where L_x and L_y are zonal and meridional scales. This leads to

$$F_m^{\text{Kelvin}}(x, t) = [(\beta/c_m\pi)^{1/2} \int_{-\infty}^{\infty} dy \exp(-\beta y^2/2c_m) \times Y(y/L_y)] \int_m^0 S(t)X(x/L_x) \quad (10)$$

where $f_m^0 = G'_m(0)(\rho_a/\rho)C/D$. The expression in brackets is another constant α_m specific to mode m. Now the expression (8) for $q(x, t)$ for a mode of speed c_m can be written as a convolution:

$$q(x, t) = \int_{-\infty}^{\infty} J(x, t - t')S(t')dt', \quad (11)$$

where $J(x, t) = \alpha f^0 X[(x - ct)/L_x]H(t)$, where $H(t)$ is the Heaviside step function. The function $J(x, t)$ is the impulse response function for the problem. For simplicity, we chose $X(x/L_x)$ to be the rectangle function

$$X(x/L_x) = \prod (x/L_x) = \{1; |x| < L_x/2, 0; |x| > L_x/2\}. \quad (12)$$

Since disturbances propagate eastward with speed c, $J(x, t)$ is zero for 1) longitudes west of the forcing region ($x < -L_x/2$) for all time and 2) for longitudes east of the western edge of the forcing region for times for which the disturbance has yet to reach or has already propagated past to the east.

Since the Fourier transform of a convolution of two functions is equal to the product of their transforms, (11) can be written as

$$\hat{q}(x, \omega) = \hat{S}(\omega)\hat{J}(x, \omega), \quad (13)$$

where carets denote transforms in time and ω is (cyclical) frequency. Noting that sea level can be computed from pressure at $z = 0$, we can use (13) to find the relation between sea level and wind for a particular mode:

$$\hat{\eta}(x, \omega) = \frac{\hat{p}(x, \omega)G'_m(0)}{g} = \frac{\hat{q}(x, \omega)G'_m(0)c_m}{2g}. \quad (14)$$

Finally, the total admittance for all modes together at latitude y is

$$\hat{a}(x, y, \omega) = \hat{\eta}/\hat{S}(\omega) = \sum_{m=1}^{\infty} \frac{\hat{J}_m(x, \omega)G'_m(0)c_m}{2g} \exp(-\beta y^2/2c_m). \quad (15)$$

Since we are interested in a location x inside the forcing patch, the Fourier transform of $J(x, t)$ becomes

$$\hat{J}_m(x, \omega) = \frac{\alpha_m f_m^0}{c_m}(x + \tfrac{1}{2}L_x) \frac{\sin[\pi(x + \tfrac{1}{2}L_x\omega/c_m]}{\pi(x + \tfrac{1}{2}L_x)\omega/c_m} \times \exp[-2\pi i(x + L_x/2)\omega/c_m]. \quad (16)$$

FIG. 9. Observed and model Kelvin-wave admittance between local east pseudo-stress and sea level: (a) $\hat{a}(x, y, \omega)$ for each of the lowest three baroclinic modes evaluated at the equator with $L_x = 10^3$ km, $L_y \to \infty$. (Sharp phase shifts should be vertical lines, but are not drawn that way because of finite frequency resolution.) (b) $a(x, y, \omega)$ summed over up to the lowest 9 baroclinic modes evaluated at the equator with $L_x = 10^3$ km, $L_y \to \infty$. (c) Observed admittance $a(\omega)$ at Beru and $a(x, y, \omega)$ summed over up to the lowest 9 baroclinic modes evaluated at the latitude of Beru with $L_x = 10^3$ km, $L_y = 450$ km.

The constants α_m are determined by how well the meridional shape of the wind projects onto the basis functions $\exp(-\beta y^2/2c_m)$. Again for simplicity, we take $Y(y/L_y)$ to be a Gaussian shape with decay scale L_y centered at latitude y_0. Then

$$\alpha_m = (\beta/c_m\pi)^{1/2} \int_{-\infty}^{\infty} dy \exp(-\beta y^2 2c_m) Y(y/L_y)$$

$$= (\beta/c_m\pi)^{1/2} \int_{-\infty}^{\infty} dy \exp(-\beta y^2 2c_m) \times \exp\{-[(y - y_0)/L_y]^2\} \quad (17)$$

$$= \sqrt{2}\gamma_m^{-1} \exp[-(y_0/\gamma_m L_y)^2],$$

where $\gamma_m = (1 + 2c_m/\beta L_y^2)^{1/2}$. Eqs. (15)–(17) give a complete specification of the Kelvin-wave sea-level response of an equatorial ocean to zonal wind stress forcing. The case of interest is the one for which $\hat{J}(x, \omega)$ has been evaluated: the relevant part of the wind patch extends from its western extremity east to the observing longitude. The phase of $\hat{J}_m(x, \omega)$ in (16) corresponds to a time lag of $(x + L_x/2)/c_m$, that is, the time it takes for the trailing edge of a rectangular pulse in sea level to reach the observing longitude x. The amplitude of $\hat{J}_m(x, \omega)$ is modulated by the sinc function [$= \sin\pi x'/\pi x'$, the Fourier transform of $\prod(x')$], where the duration of the patch relevant to measurement at x is also $(x + L_x/2)/c_m$. The amplitude of each term in the sum (15) varies linearly with the effective extent of the wind patch (i.e., $x + L_x/2$) and can be weaker or stronger depending on the effectiveness of the projection of the meridional Kelvin-mode shape onto the wind structure. For large wind scales $L_y \gg \sqrt{c_m/\beta}$, $\alpha_m \to \sqrt{2}$ but for small meridional scales

$$L_y \ll \sqrt{c_m/\beta}, \quad \alpha_m \to (L_y/\sqrt{c_m/\beta}) \exp(-y_0^2\beta/2c_m).$$

Taking typical values for $\rho_a/\rho = 1.29 \times 10^{-3}$, $C = 2.5 \times 10^{-3}$, $\beta = 2.285 \times 10^{-11}$ s^{-1} m^{-1}, $g = 9.78$ m s^{-2}, $D = 5000$ m and using the c_m and $G'_m(z)$ computed from relevant buoyancy–frequency profiles, we can evaluate various admittance functions $\hat{a}(x, \omega)$. The simplest case is for $L_y \gg \sqrt{c_m/\beta}$, $y = 0$ and a zonal scale $(x + L_x/2) = 10^3$ km, shown in Fig. 9a. Phase variation is dominated by the lowest two modes, as is amplitude. For individual modes, phase changes by 180° at each node of the sinc function, as expected. The same example, extending the sum (15) successively from 1 to 9 vertical modes (Fig. 9b), indicates that for periods $\leqslant 10^3$ h, the contribution of vertical modes $\geqslant 3$ is negligible to both amplitude and phase of $\hat{a}(x, \omega)$. Varying the zonal scale $(x + L_x/2)$ produces nearly proportional changes in both admittance amplitude and rate of change of phase with frequency.

The admittance $a(\omega)$ calculated from the Beru observations (using two data pieces of 320 days each and averaging over eight adjacent frequency bands) is plotted in Fig. 9c. From the coherences in Fig. 6a, only the first six admittance estimates are significant. Observed admittances at Tarawa are similar, although coherence is lower, presumably because the wind is weaker there. Nevertheless, the admittance amplitude and phase vary in a similar manner at the two islands. Along with the Beru admittance is $\hat{a}(x, \omega)$ calculated for the appropriate latitude (1°20'S) for a wind patch centered at $y_0 = 1°20'$S with a meridional scale $L_y = 450$ km. The scale L_y was chosen by fitting the model wind structure to the lowest empirical orthogonal function structure of the observed winds. Except at periods of 5 days and shorter (where gravity waves are known to produce peaks in sea-level spectra), the agreement in both magnitude and phase is rather good.

Although the parameterization of the wind in the model is extremely crude, the fact that the theory can be tuned with relatively little trouble to reproduce the observations (Fig. 9c) suggests that the basic elements of the theory are correct; that is, linear baroclinic-mode equatorial Kelvin waves forced by a zonal wind give rise to a sea-level signal that has magnitude and phase similar to what is observed. There is really only one parameter, L_x, the zonal scale of the wind, which does not have a magnitude suggested by the wind observations alone. It is the single truly "free" parameter we can adjust, on the basis of observations, to make the model admittance mimic the observations. As noted above, varying L_x changes both the magnitude and frequency behavior of the model admittance amplitude and phase simultaneously, so that a single free parameter is being used to fit two independent features of the observations for each frequency. The meridional shape and scale of the wind is also crude, but the parameters y_0 and L_y follow from the observations once the (probably highly oversimplified) Gaussian shape has been chosen. Substantially different choices of any of the parameters either disagree grossly with what is known about the wind, or lead to substantially different magnitude and frequency behavior of both model admittance and phase.

The model we have presented ignores friction, but it is easy to assess the effect friction would have on zonal wind–sea level admittance. Mofjeld (1981) considers the effect of Rayleigh friction on equatorial waves, noting that different vertical modes decouple only if viscosity varies inversely with stability, a rather special requirement. His solutions indicate that Kelvin waves propagate more slowly with friction than without (in contrast to the observations discussed here, in which disturbances travel faster than inviscid theory predicts). Another Kelvin-wave property is that zonal current and vertical displacement are out of phase by $\delta/2\omega$ for $\delta \ll \omega \ll (\beta c)^{1/2}$ where δ is the friction and ω, β and c are as employed earlier. Mofjeld quotes $\delta^{-1} = 34$ days as being a representative

value in observational studies, putting the frequency range we are considering in the observations between the limits stated for $\delta/2\omega$ to be the phase between current and displacement. For ω = 1–3 cycles per 40 days, $\delta/2\omega \approx$ 2–5°, which, compared to the admittance phases in Fig. 9c is small and of the wrong trend (i.e., varying inversely with rather than proportionally to ω). (The phase between zonal current and vertical displacement in the frictional model is presumably linked to the phase between zonal wind forcing and sea level.) Thus, the effects of friction appear to run counter to the observations both of zonal speed and wind stress–sea level admittance phase. This particular frictional model does not seem to be relevant to our observations.

7. Discussion and conclusions

The fluctuations in sea level at periods of a few weeks observed coherently at island stations in the western and eastern Pacific can be explained as low (first) baroclinic-mode equatorial Kelvin waves. These waves appear modified by currents to travel faster than predicted by linear perturbations to a resting ocean. The primary evidence for Kelvin waves at these periods is the clear tendency for eastward propagation of phase (Fig. 2) at a speed not far from what is predicted by linear theory. This signal was first documented by Luther (1980) for a 35–80 period band. A particular realization of this process was discussed by Knox and Halpern (1982). Eriksen (1982b) computed a frequency–zonal-wavenumber spectrum for sea-level fluctuations at islands from Nauru to Canton, finding that in low-frequency bands other than those contaminated by tides (e.g., the lunar fortnightly tide), there is a clear tendency for eastward wavenumbers. The other evidence that sea-level fluctuations are a manifestation of low (primarily the first) baroclinic-mode Kelvin waves is coherence between sea level and deep temperature fluctuations at Beru and Abemama (see Eriksen, 1982b) and coherence and spectral-density meridional variation at the Galápagos Islands (Ripa and Hayes, 1981) consistent with the predictions of simple linear theory.

The behavior of coherence phase with frequency of sea level at different zonal separations indicates that phase travels about 16% faster than what linear theory would predict. Schematic models of equatorial-undercurrent influence on equatorial waves (McPhaden and Knox, 1979; Philander, 1979) show that Kelvin waves should travel somewhat faster than in a resting ocean (i.e., 10–25% faster). Ripa and Marinone (1983) show that the effective value of the current is an average weighted with the square of the Kelvin wave function. Therefore, in a continuous model (where wave structure is not restricted to take the same form as mean currents, as it is in one-layer models) the equatorial undercurrent does not account for such a large increase in wave speed. Calculations of Kelvin-wave self-interaction (Ripa, 1982), however, show that Kelvin waves of moderate amplitude [O(10 cm) *positive* sea level changes] induce an increase in zonal speed comparable to what is observed; a Kelvin wave associated with a sea surface *depression,* however, produces a decrease in the propagation speed. Knox and Halpern (1982) observed what amounts to a realization of a Kelvin wave (a nearly non-dispersive disturbance) in upper-ocean integrated current to travel at 15–18% faster than the linear speed. This result is consistent with the statistical result we find over different (larger) zonal separations in examining records roughly one year in length.

The wind records from Butaritari, Tarawa and Beru indicate that low-frequency fluctuations have substantial variability on meridional scales comparable to those of low-mode baroclinic equatorial waves in the ocean. Zonal-wind-energy density changes by an order of magnitude over a meridional separation of nearly 500 km at periods of a few weeks. These zonal-wind fluctuations are coherent over meridional separations of up to 300 km, but only marginally coherent at larger separations. Meridional wind is at most marginally coherent at any of the separations available. The implication of meridional structure of wind on these scales for baroclinic ocean waves is that they will be excited more or less efficiently depending on how large the meridional scale of the wind is (except in the special case that it takes on structure resonant with particular meridional ocean modes). Some part of the variability at these periods seems due to cyclone pairs that develop on each side of the equator and may or may not translate in the same direction (Sadler and Kilonsky, 1981; Keen, 1982). Zonal scales may be somewhat longer, since wind events at Banaba (formerly called Ocean Island), occur at nearly the same time as at Beru, some 750 km to the east (Luther, personal communication, 1982).

Zonal winds appear to generate the oceanic disturbances identified as Kelvin waves. There is coherence not only between east pseudo-stress and local sea level, but also between it and remote sea level to the east over a separation amounting to more than a quarter of the earth's circumference. As discussed in Section 5, there is a time lag of about 2.5 days between zonal pseudo-stress and local sea level at Beru. In the model in Section 6, this lag was associated with a zonal length scale of 1000 km, assuming a hypothetical zonal structure for the wind. At Canton 1100 km farther to the east, the time lag between zonal wind and sea level appears to be nearly 5 days, according to the coherence computed for 1954–58 (Wunsch and Gill, 1976, Fig. 7c). Luther (personal communication, 1982) suggests that reversals in the direction of the wind for a few days (as shown in Fig.

2) occur much less frequently at Canton than in the Gilbert Group. There are also interannual changes in the frequency of these events (Luther, Harrison and Knox, personal communications, 1982). The model of the previous section suggests a zonal scale for the wind of 2000 km to find the 5-day lag between wind and local sea level. The reversals in wind direction probably dominate the variance in zonal wind at periods of a few weeks, so that wind-stress events which emanate from the west of the Gilbert Group to reach Canton plausibly have larger scale than those at Beru. [Westerly wind events are more common in the Gilbert Group than at Canton (Luther, personal communication, 1982).] Luther (1980) computed eastwind–sea level coherence at Canton for a 16.5-year record to find no obvious phase lag in the period range of ~1–6 weeks. Our model suggests that a definitive phase lag is the result of a predominant zonal scale of wind disturbances. Perhaps, over many years [particularly over non-El Niño years according to Luther (personal communication, 1982)], there may be no particular preferred zonal scale to the wind, thus destroying the phase lag in long records.

Although the admittance function we calculate from the model suggests that the first two baroclinic modes account for the majority of Kelvin-wave sea-level variance excited by a zonal wind, the observations do not show clear evidence of baroclinic modes other than the first. For instance, there is no recognizable similarity between sea level at Abemama and that at N. Isabela 67 days later (a time lag corresponding to the second baroclinic mode as opposed to 41 days for the first). It may be that the second baroclinic mode is attenuated substantially in its propagation compared to the first mode, or never even excited. This is a discrepancy between the observations and our theory. Moored measurements of current and temperature structure may be needed to detect the mixture of modes present.

Acknowledgments. The authors thank D. Luther for helpful comments in reviewing this work and extend their gratitude to R. Reid of C. S. Draper Laboratory, G. Brown of MIT, the officers and crew of MV *Tautunu,* and the government of the Republic of Kiribati for their help in carrying out field work in the Gilbert Islands. We thank N. N. Soreide and B. Davies of PMEL, H. Miller of the University of Washington, the Director and staff of the Charles Darwin Research Station, and the Instituto Oceanografica de la Armada (INOCAR) of Ecuador for their help in obtaining the measurements at the Galápagos Islands.

This work was supported by the National Science Foundation under Grant OCE-79-21816 and by the Equatorial Pacific Ocean Climate Studies Project of NOAA under Grant RP0000/8C692021. This is PEQUOD (Pacific Equatorial Ocean Dynamics project) Contribution Number 22.

REFERENCES

Bendat, J. S., and A. G. Piersol, 1971: *Random Data: Analysis and Measurement Procedures.* Wiley-Interscience, 407 pp.

Cane, M. A., and E. S. Sarachik, 1976: Forced baroclinic ocean motions. I. The linear equatorial unbounded case. *J. Mar. Res.*, **34,** 629–665.

Eriksen, C. C., 1980: Evidence for a continuous spectrum of equatorial waves in the Indian Ocean. *J. Geophys. Res.*, **85,** 3285–3303.

——, 1981: Deep currents and their interpretation as equatorial waves in the western Pacific Ocean. *J. Phys. Oceanogr.*, **11,** 48–70.

——, 1982a: Geostrophic equatorial deep jets. *J. Mar. Res.*, **40** (suppl), 143–157.

——, 1982b: Equatorial wave vertical modes observed in a western Pacific island array. *J. Phys. Oceanogr.*, **12,** 1206–1227.

Gill, A. E., and A. J. Clarke, 1974: Wind-induced upwelling, coastal currents and sea-level changes. *Deep-Sea Res.*, **21,** 325–345.

Hayes, S. P., J. Glenn and N. Soreide, 1978: A shallow water pressure-temperature gauge (PTG): Design, calibration and operation. Tech. Memo. PMEL-ERL, NOAA, Seattle, WA.

Keen, R. A., 1982: The role of cross-equatorial cyclone pairs in the Southern Oscillation. *Mon. Wea. Rev.*, **110,** 1405–1416.

Knox, R. A., and D. Halpern, 1982: Long range Kelvin wave propagation of transport variations in Pacific Ocean equatorial currents. *J. Mar. Res.*, **40** (suppl), 329–339.

Koopmans, L. H., 1974: *The Spectral Analysis of Time Series.* Academic Press, 366 pp.

Luther, D. S., 1980: Observations of long period waves in the tropical oceans and atmosphere. Ph.D. thesis, MIT-Woods Hole Oceanographic Institution Joint Program in Oceanography.

McPhaden, M. J., and R. A. Knox, 1979: Equatorial Kelvin and inertia-gravity waves in zonal shear flow. *J. Phys. Oceanogr.*, **9,** 263–277.

Mofjeld, H. O., 1981: An analytic theory on how friction affects free internal waves in the equatorial waveguide. *J. Phys. Oceanogr.*, **11,** 1585–1590.

Philander, S. G. H., 1979: Equatorial waves in the presence of the equatorial undercurrent. *J. Phys. Oceanogr.*, **9,** 254–262.

Ripa, P., 1982: Nonlinear wave–wave interactions in a one-layer reduced-gravity model on the equatorial β plane. *J. Phys. Oceanogr.*, **12,** 97–111.

——, and S. P. Hayes, 1981: Evidence for equatorial trapped waves at the Galapagos Islands. *J. Geophys. Res.*, **86,** 6509–6516.

——, and S. G. Marinone, 1983: The effect of zonal currents on equatorial waves. *Hydrodynamics of the Equatorial Ocean,* J. Nihoul, Ed., *Elsevier Oceanographic Series* Vol. 36, 291–317.

Sadler, J. C., and B. J. Kilonsky, 1981: Meteorology during the test shuttle experiment. University of Hawaii, Dept. Meteor., Tech. Rep. UHMET 81-05, Honolulu.

Tajchman, S. J., 1981: Comments on measuring turbulent exchange within and above forest canopy. *Bull. Amer. Meteor. Soc.*, **62,** 1550–1559.

Wunsch, C., 1972: Bermuda sea level in relation to tides, weather, and baroclinic fluctuations. *Rev. Geophys. Space Phys.*, **10,** 1–49.

——, and J. Dahlen, 1974: A moored temperature and pressure recorder. *Deep-Sea Res.*, **21,** 145–154.

——, and A. E. Gill, 1976: Observations of equatorially trapped waves in Pacific sea level variations. *Deep-Sea Res.*, **23,** 317–390.